Fluorescence Anisotropy as a Method to Examine the Thermodynamics of Enantioselectivity

Yafei Xu and Matthew E. McCarroll*

Department of Chemistry and Biochemistry, Southern Illinois University, Carbondale, Illinois 62901

Received: December 9, 2004; In Final Form: February 16, 2005

A new method is evaluated whereby enantioselective binding is examined by use of steady-state fluorescence anisotropy measurements. A theoretical treatment is presented that relates fluorescence anisotropy measurements to chiral selectivity and allows the estimation of thermodynamic parameters of chiral recognition. It is shown that the natural logarithm of the ratio of anisotropy values of two enantiomers varies as a function of temperature in a manner where the slope and intercept are directly related to the differential enthalpy ($\Delta\Delta H°$) and entropy ($T\Delta\Delta S°$) of the enantioselective interaction. The developed method was evaluated by examining the enantioselective interactions of several chiral molecules with β-cyclodextrin and a molecular micelle.

Introduction

Chiral recognition is a fundamental phenomenon that is observed in all biological systems, ranging from single-cell organisms to the most complex of animals. In fact, the specificity and efficacy of many biologically important reactions are based on chiral interactions.[1,2] Hence, biological activity depends on the enantiomeric form of the compound, not simply the chemical structure. Since a 1992 mandate by the Federal Food and Drug Administration, producers of pharmaceuticals have been required to evaluate the effects of individual enantiomers and verify the enantiomeric purity of chiral drugs that are produced. Additionally, the pharmaceutical properties and toxicity must be established independently for both enantiomers, even if the drug is to be marketed as a single enantiomer. This has resulted in an increased need for techniques to evaluate chiral interactions and methods for determining enantiomeric purity, as well as preparative-scale enantiomeric separations. Originally, efforts in the development of chiral drugs were targeted at identifying and isolating deleterious effects due to the presence of the other enantiomer. Recent developments, however, have focused on the enantioselective interactions of chiral drugs as a development tool to increase the efficacy and specificity of pharmaceuticals.[1]

Various techniques have been used to study chiral recognition, including microcalorimetry, UV−visible absorption spectroscopy, fluorescence spectroscopy, nuclear magnetic resonance, mass spectrometry, thermal analysis, and various chromatographic or electrophoretic methods.[3−21] These studies have contributed to a body of knowledge pertaining to chiral interactions and the measurement thereof, yet a critical need still exists for the development of more sensitive and facile methods of examining the subtle phenomenon of chiral recognition.

In this regard, we have undertaken studies examining the use of fluorescence spectroscopy as a tool in the study of chiral interactions, following preliminary observations that have been published.[22] Various fluorescence techniques have been used in chiral recognition studies,[22−33] including studies based on fluorescence intensity, spectral shifts, fluorescence polarization, fluorescence lifetimes, fluorescence resonance energy transfer, and fluorescence quenching. Recently, Al Rabaa et al.[25] reported the spectroscopic characterization of a chiral anthryl probe and its interactions with DNA. In 2001, a preliminary study published by McCarroll et al.[22] detailed the use of fluorescence polarization to study chiral interactions specifically. These two papers represent the first published efforts to use anisotropy as a measure of chiral recognition. Recently, we reported the determination of enantiomeric composition using fluorescence anisostopy.[34]

Fluorescence anisotropy measurements can provide useful information for host−guest interactions.[35] When fluorescent enantiomers are bound to a chiral selector, the anisotropy will reflect the overall rotation of the complex as well as any segmental motion independent of the overall rotation. Additionally, any differences in the fluorescence lifetimes will affect the anisotropy value. Because polarization effects are additive, the observed steady-state anisotropy is the weighted average of the contributions of segmental motion and the distribution between free and bound species. For a given host−guest system, the anisotropy of a guest molecule is dependent on the degree of interaction between the guest and the host. In the case of chiral recognition, one enantiomer will have a stronger interaction, resulting in a higher anisotropy. Importantly, preliminary results indicate that the difference in anisotropy between two enantiomers is well correlated to chiral recognition.[22]

Native and modified cyclodextrins (CDs) have been widely studied as host systems in terms of molecular interactions and chiral recognition.[36−41] A characteristic of CDs as chiral selectors is their ability to form stereoselective inclusion complexes with a wide variety of chiral molecules via noncovalent interactions.[40] Consequently, cyclodextrins can serve as excellent models for understanding inclusion complexation and chiral recognition processes.[5,6,42]

In this work, steady-state fluorescence anisotropy was used to study host−guest complexation, chiral recognition, and the thermodynamics of these processes. A theoretical framework is presented that allows the estimation of the thermodynamic parameters of chiral recognition. To evaluate the method and guide future development, the temperature-dependent fluorescence anisotropy was examined for eight chiral compounds in the presence of the chiral selector β-cyclodextrin (Scheme 1A). In addition, results from a second test case are presented where

* Corresponding author. E-mail: mmccarroll@chem.siu.edu.

10.1021/jp044380c CCC: $30.25
Published on Web 03/29/2005

SCHEME 1: Depiction of Enantioselective Binding with the Chiral Selectors *β*-Cyclodextrin (A) and Poly(sodium undecanoyl-L-valinate) (B) That Were Examined in This Study

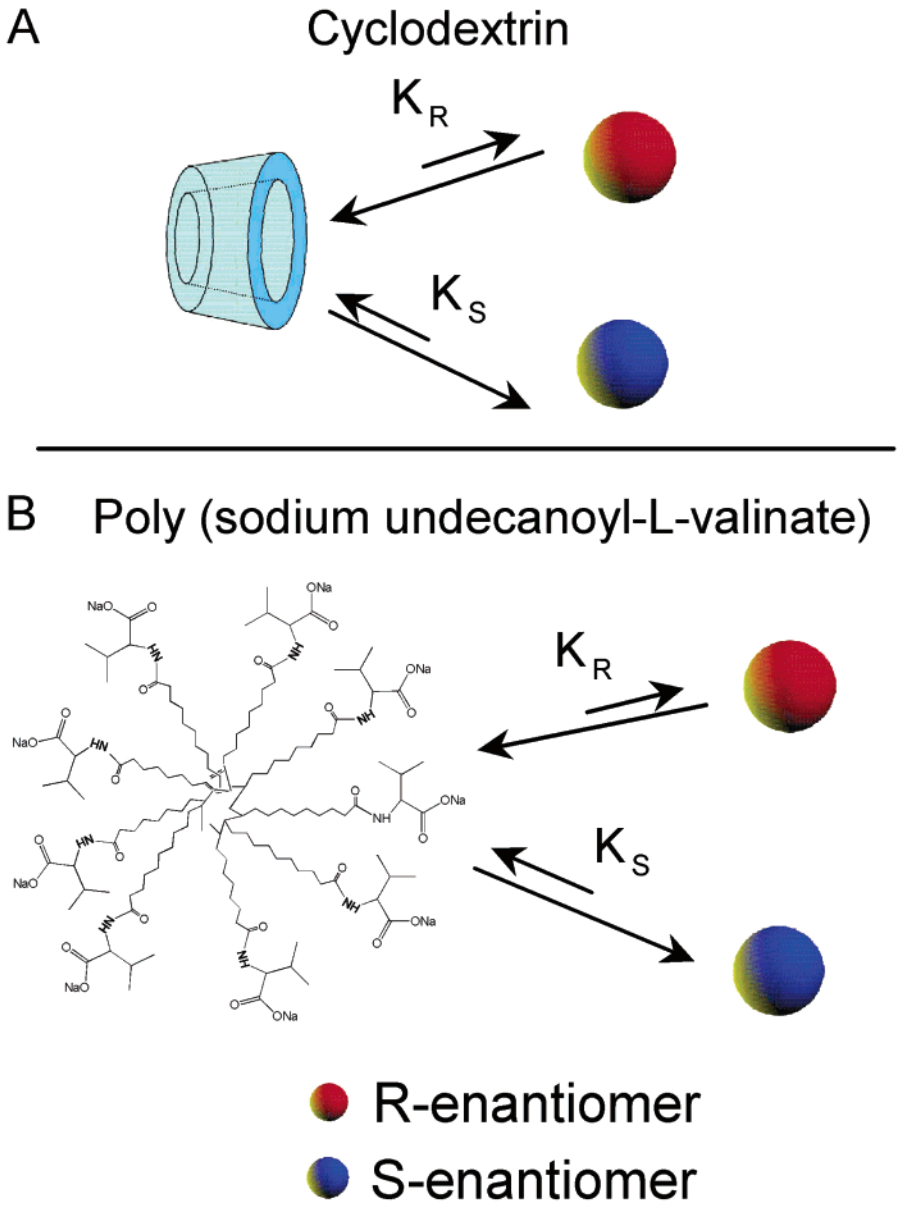

the interactions of four chiral compounds and a chiral molecular micelle are examined (Scheme 1B).

Experimental Section

Materials. *β*-Cyclodextrin (CD) was a gift from Cerestar USA, Inc. (Hammond, IN). *O*,*O*′-Dibenzoyl tartaric acid (DBTA), *N*-acetyl tryptophan, phenylalanine methyl ester (PAME), and mandelic acid were obtained from Sigma-Aldrich Co. (St. Louis, MO). Propranolol, tryptophan, binaphthyl-2,2′-diylhydrogenphosphate (BNP), [1,1′-binaphthalene]-2,2′-diamine (BNA), and [1,1′-binaphthalene]-2,2′-diol (BOH) were purchased from Aldrich Chemical Co. (Milwaukee, WI). In the case of all chiral compounds, the pure enantiomers were purchased and used as received. Water used in all experiments was purified by a Milli-Q system (Millipore Inc., Milford, MA) to a resistance of at least 18 MΩ. All chemicals were used as received. The molecular micelle poly(sodium undecanoyl-L-valinate) (PSUV) was synthesized and polymerized following a procedure developed in Professor Isiah Warner's laboratory at Louisiana State University.[43]

Fluorescence Anisotropy Measurements. A modular spectrofluorometer (Photon Technology International Inc., New Jersey) equipped with double monochromators and a photon-counting PMT detector was used for all fluorescence anisotropy measurements. The instrument is equipped with large-aperture Glann-Thompson polarizers for the anisotropy experiments. All fluorescence anisotropy measurements were corrected for instrumental polarization bias using *G*-factor correction. A Xe lamp was used as an excitation source for each of the analytes examined (BNA = 318 nm, BNP = 324 nm, BOH = 333 nm, PAME = 280 nm, propranolol = 290 nm, tryptophan = 300 nm, acetyltryptophan = 300 nm, and mandelic acid = 280 nm). The measurement temperature was controlled and adjusted using a thermocirculator (NESLAB Instruments, Inc., Newington, NH), and 1-cm quartz cuvettes were used for all fluorescence measurements. The data analysis was performed by least-squares analysis with the program Kaleidagraph (Synergy Software, Reading, PA).

Capillary Electrophoretic Measurements. Capillary electrophoresis experiments were carried out with a Beckman MDQ

CE system equipped with a UV detector (detection wavelength 214 nm). A 60-cm-long capillary (50-cm effective length, 50-μm i.d., Polymicro Technologies, LLC, Phoenix, AZ) was used for CE separations. Separations were carried out using hydrodynamic injection (0.2 psi for 2 s) and a separation voltage of 25 kV. The background electrolyte consisted of a 50 mM mixture of NaH_2PO_3 and Na_2HPO_3 buffered at pH 4.8 or 6.9 with the addition of an appropriate amount of chiral selector. All electrolyte solutions were filtered through a 0.45-μm syringe filter and degassed by sonication. The capillary was conditioned by rinsing sequentially with 0.10 M NaOH, deionized water, and running buffer for 20 min at the beginning of each day.

Solution Preparation. Solutions used in this study were prepared with aqueous phosphate or acetate buffers (50 mM, pH 7.0 and 4.8). Sample concentrations ranged from 10 to 50 μM.; β-CD solutions were prepared by dissolving solid CDs in phosphate or acetate buffer (11 mM). PSUV solutions were prepared in a borate buffer (pH 9.0, 0.5%). Before measurement, the solutions were mixed by sonication for ~20 min and allowed to equilibrate for at least 30 min.

Theory

Fluorescence Anisotropy. Fluorescence polarization is frequently expressed in terms of anisotropy (r) because of the comparatively simple equations describing rotational depolarization. The dependence of fluorescence anisotropy on molecular rotation can be described quantitatively with the well-known Perrin equation,[35]

$$\frac{r_0}{r} = 1 + \frac{\tau}{\phi} \tag{1}$$

where τ is the lifetime and ϕ is the rotational correlation time. The magnitude of the anisotropy depends on the rotational correlation time (ϕ). Therefore, a relatively small fluorophore bound to a large, more slowly rotating macromolecule (large ϕ) will display a higher anisotropy value. In the case of host−guest interactions, an analyte generally exists in one of two forms, the bound complex or the free species. Thus, the total anisotropy for the binding system is a weighted average of the anisotropy values of the bound species and free analyte.[35] The anisotropy of a small fluorophore rotating freely in solution typically approaches zero because of rapid rotational depolarization, and the contribution from free analyte to the measured anisotropy is negligible. Under these circumstances, the total anisotropy of the system mainly depends on the anisotropy of the bound species and the fractional distribution. As a result, the measured anisotropy can be taken as a measure of the fraction of host-bound analyte, which in turn is indicative of the stability of the host−guest complex (i.e., binding constant). An additional, albeit subtle, effect results from any differences between the rotational motion of the bound analyte and the chiral selector. For example, the bound form of the more weakly binding enantiomer will likely exhibit a larger degree of segmental motion.

Thermodynamic Considerations. For a given host−guest complexation system, the association can be represented by

$$A + S \leftrightarrow AS \tag{2}$$

where A represents a guest molecule (analyte) and S represents a host molecule (selector). The guest molecules may exist in the form of a bound complex (A−S) or the free species (A). The measured anisotropy (r_{av}) is the weighted average of the anisotropy values of the bound (r_b) and free analyte (r_f), where the contribution is determined by the fractional fluorescence intensity from the bound (f_b) and free (f_f) species.

$$r_{av} = f_b r_b + f_f r_f \tag{3}$$

Assuming fractional intensity corresponds to population distributions, the fraction of the bound species can be expressed in terms of the concentrations of the complexed and free forms of the analyte (eq 4).

$$f_b = \frac{[AS]}{[AS] + [A]} \tag{4}$$

Considering the expression of the association constant of the complexation reaction,

$$K = \frac{[AS]}{[A][S]} \tag{5}$$

eq 4 can be arranged to represent the fraction of the bound species in terms of the binding constant, K,

$$f_b = \frac{[AS]}{[AS] + [A]} = \frac{K[S]}{K[S] + 1} \tag{6}$$

and

$$f_f = 1 - f_b = 1 - \frac{K[S]}{K[S] + 1} \tag{7}$$

Incorporation of eqs 6 and 7 into eq 3 results in

$$r_{av} = r_b \frac{K[S]}{(K[S] + 1)} + r_f \left[1 - \frac{K[S]}{(K[S] + 1)}\right] \tag{8}$$

which relates the average anisotropy to the anisotropy of the bound species, the binding constant, and the concentration of the selector. Because r_f usually approaches zero, eq 8 can often be approximated by

$$r_{av} = r_b \frac{K[S]}{(K[S] + 1)} \tag{9}$$

Many factors affect the average anisotropy value in a given system, only some of which are enantioselective. Fortunately, nonenantioselective factors affect both enantiomers equally and do not lead directly to a difference in anisotropy values between two enantiomers. To examine the enantioselectivity specifically, we can examine the ratio of the anisotropy values (eq 10).

$$\frac{r_{av,R}}{r_{av,S}} = \frac{r_{b,R} K_R[S]}{K_R[S] + 1} \cdot \frac{K_S[S] + 1}{r_{b,S} K_S[S]} \tag{10}$$

Equation 10 can be arranged to the form of eq 11,

$$\frac{r_{av,R}}{r_{av,S}} = \frac{r_{b,R}}{r_{b,S}} \cdot \frac{K_R}{K_S} \cdot \frac{(K_S[S] + 1)}{(K_R[S] + 1)} \tag{11}$$

which shows the dependence of the ratio of the anisotropy values to the differences in the anisotropy of the bound species, the binding constants, and the concentration of free selector. It should be noted that the first and last terms of the equation will typically approach unity, hence the ratio of the binding constants (i.e., selectivity) is the primary factor expected to lead to differences in the measured anisotropy values of the two enantiomers.

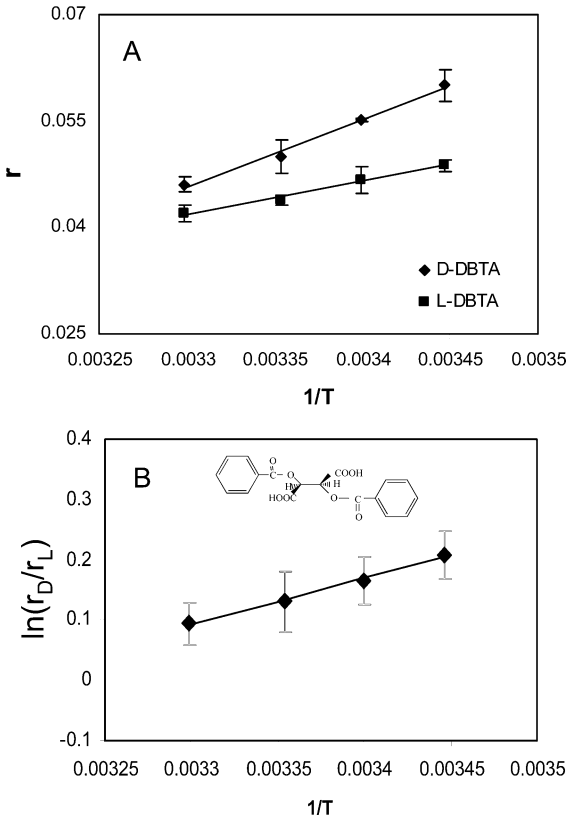

Figure 1. Temperature-dependent fluorescence anisotropy of the enantiomers of O,O′-dibenzoyl tartaric acid (DBTA) in the presence of β-cyclodextrin shown as the anisotropy values (A) and the natural logarithm of the ratio of anisotropy values for the enantiomers (B).

Because a relationship exists between the anisotropy and the binding constants, the thermodynamics of the enantioselective binding can be evaluated. It is well established that the Gibbs free energy for complex formation can be related to the binding constant by

$$\Delta G^\circ = -RT \ln K \tag{12}$$

where ΔG° is the Gibbs free energy for the formation of the complex. Furthermore, it is known that the differential free energy of enantioselective binding is given by

$$\frac{\Delta\Delta G^\circ_{R,S}}{-RT} = \ln\left(\frac{K_R}{K_S}\right) = \frac{-\Delta\Delta H^\circ}{RT} + \frac{\Delta\Delta S^\circ}{R} \tag{13}$$

Evaluating the logarithm of eq 11 results in

$$\ln\left(\frac{r_{av,R}}{r_{av,S}}\right) = \ln\left(\frac{K_R}{K_S}\right) + \ln\left(\frac{r_{b,R}}{r_{b,S}}\right) + \ln\left(\frac{(K_S[S]+1)}{(K_R[S]+1)}\right) \tag{14}$$

which allows substitution of the $\Delta\Delta G^\circ$ term from eq 13, resulting in the useful form shown in eq 15.

$$\ln\left(\frac{r_{av,R}}{r_{av,S}}\right) = \frac{-\Delta\Delta H^\circ}{RT} + \frac{\Delta\Delta S^\circ}{R} + \ln\left(\frac{r_{b,R}}{r_{b,S}}\right) + \ln\left(\frac{(K_S[S]+1)}{(K_R[S]+1)}\right) \tag{15}$$

The differential fluorescence anisotropy is thus dependent on the thermodynamics of the enantioselective interaction and the anisotropy of the bound species. The difference in the anisotropy values of the bound species is indicative of the diastereomeric complexes (i.e., chiral recognition), whereas the difference in binding constants is a thermodynamic consequence of chiral recognition. The terms $\ln(r_{b,R}/r_{b,S})$ and $\ln((K_S[S] + 1)/(K_R[S] + 1))$ will approach zero, and the differences observed in the steady-state anisotropy measurements are primarily a result of the distribution between free and bound species. A plot of $\ln(r_{av,R}/r_{av,S})$ versus $1/T$ results in a response where the slope is equal to $\Delta\Delta H^\circ/R$ and the intercept is equal to $\Delta\Delta S^\circ/R$ plus a constant that approaches zero. In cases where the constant is not negligible, the response should remain linear with a bias to the intercept.

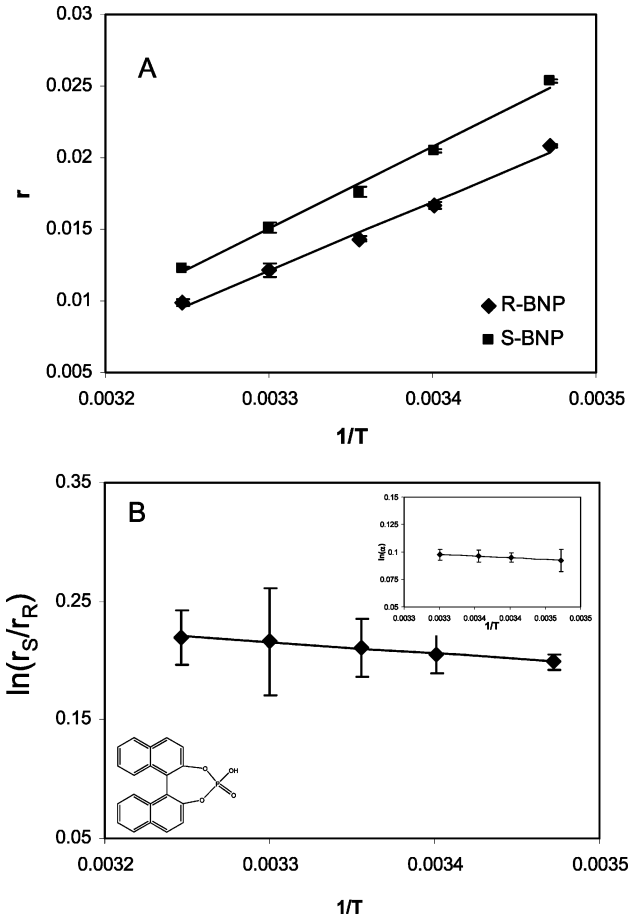

Figure 2. Temperature-dependent fluorescence anisotropy of the enantiomers of BNP in the presence of β-cyclodextrin shown as the anisotropy values (A) and the natural logarithm of the ratio of anisotropy values for the enantiomers (B).

TABLE 1: Thermodynamic Parameters of Enantioselective Binding with β-Cyclodextrin Determined from the Temperature-Dependent Fluorescence Anisotropy

compound	$\Delta\Delta H^\circ$ (kJ mol^{-1})	$T\Delta\Delta S^\circ$ (kJ mol^{-1})	$\Delta\Delta G^\circ$ (kJ mol^{-1})
DBTA	-6.37 ± 0.34	-6.04 ± 0.34	-0.33 ± 0.48
BNP	0.785 ± 0.054	1.31 ± 0.05	-0.52 ± 0.08
BNA	2.81 ± 0.58	3.18 ± 0.58	-0.37 ± 0.82
BOH	5.47 ± 1.49	5.71 ± 1.50	-0.24 ± 2.12
tryptophan	-3.67 ± 0.14	-3.50 ± 0.14	-0.17 ± 0.20
N-acetyltryptophan	-2.27 ± 0.50	-1.93 ± 0.50	-0.34 ± 0.71
PAME	-3.56 ± 0.24	-3.33 ± 024	-0.23 ± 0.34
propranolol	10.80 ± 0.81	11.18 ± 0.81	-0.36 ± 1.15

TABLE 2: Thermodynamic Parameters of Enantioselective Binding with PSUV Determined from the Temperature-Dependent Fluorescence Anisotropy

compound	$\Delta\Delta H^\circ$ (kJ mol^{-1})	$T\Delta\Delta S^\circ$ (kJ mol^{-1})	$\Delta\Delta G^\circ$ (kJ mol^{-1})
DBTA	-1.264 ± 0.119	-1.142 ± 0.119	-0.122 ± 0.168
mandelic acid	-1.304 ± 0.139	-1.213 ± 0.141	-0.091 ± 0.198
PAME	-1.949 ± 0.212	-1.753 ± 0.213	0.196 ± 0.300
propranolol	-1.157 ± 0.071	-1.040 ± 0.072	-0.117 ± 0.101

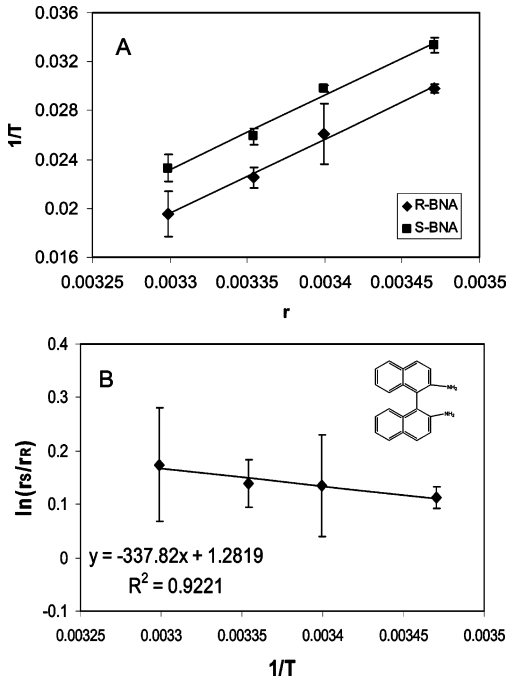

Figure 3. Temperature-dependent fluorescence anisotropy of the enantiomers of BNA in the presence of β-cyclodextrin shown as the anisotropy values (A) and the natural logarithm of the ratio of anisotropy values for the enantiomers (B).

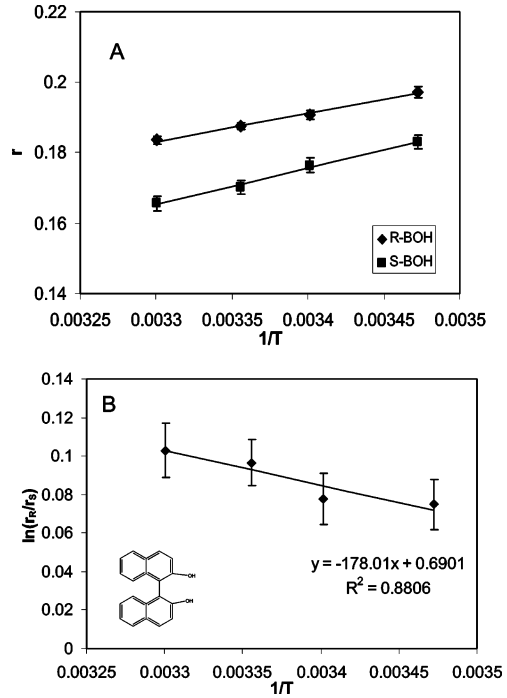

Figure 4. Temperature-dependent fluorescence anisotropy of the enantiomers of BOH in the presence of β-cyclodextrin shown as the anisotropy values (A) and the natural logarithm of the ratio of anisotropy values for the enantiomers (B).

Results and Discussion

To evaluate the aforementioned theoretical development, we have examined the temperature dependence of the enantioselective interactions of several chiral compounds with β-cyclodextrin and an amino acid-based molecular micelle as chiral selectors. Plots of $\ln(r_R/r_S)$ as a function of $1/T$ are used to infer the entropy and enthalpy from the intercept and slope, respectively. The results are shown in Tables 1 and 2, and specific examples are discussed in further detail (vide infra).

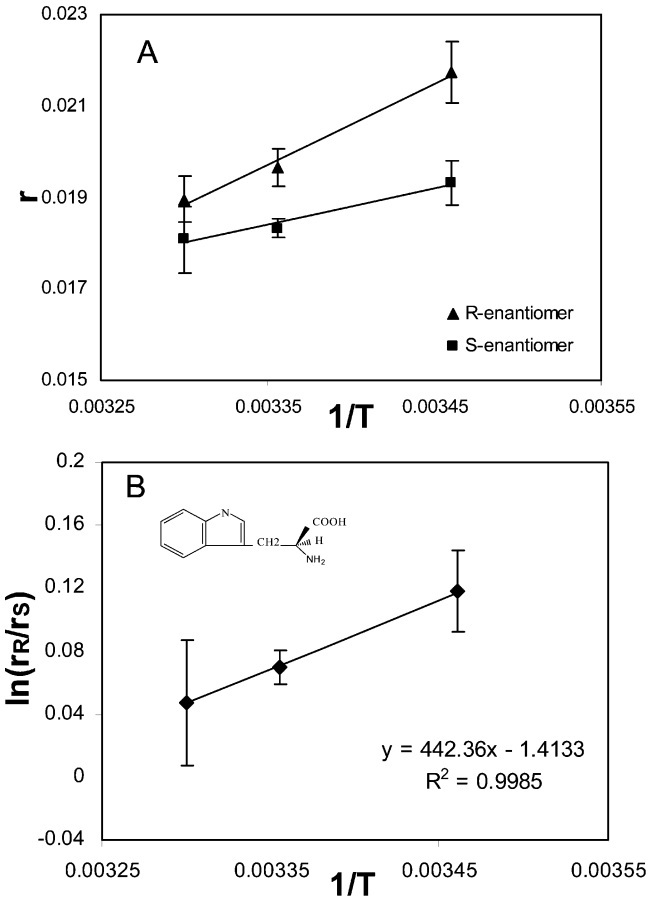

Figure 5. Temperature-dependent fluorescence anisotropy of the enantiomers of tryptophan in the presence of β-cyclodextrin shown as the anisotropy values (A) and the natural logarithm of the ratio of anisotropy values for the enantiomers (B).

***β*-Cyclodextrin.** Figure 1a shows the temperature dependence of the anisotropy of the enantiomers of O,O′-dibenzoyl tartaric acid (DBTA) in the presence of β-CD. An examination of the plot shows that significant differences in the fluorescence anisotropy of the enantiomers are observed throughout the temperature range examined and that the differences (chiral discrimination) are greater at lower temperatures. It is tempting to infer thermodynamic binding parameters directly from Figure 1a, but it must be realized that the anisotropy is a function of temperature-dependent Brownian rotation and viscosity changes in addition to thermodynamically driven changes in binding. Nevertheless, it is possible to assess the effect of temperature variation on the fluorescence anisotropy qualitatively. For example, both DBTA enantiomers display positive slopes, suggesting that the binding strengths increase with decreasing temperature. However, the D enantiomer shows a more positive slope than the L counterpart, implying a more favored enthalpy change upon complexation. This correlates well to chromatographic data showing greater interaction (chiral recognition) between β-CD and D-DBTA in the evaluated temperature range (data not shown). Figure 1b shows the plot of the natural logarithm of the ratio of anisotropy values as a function of reciprocal temperature (i.e., linear representation of eq 15). This representation of the data accounts for nonenantioselective artifacts (viscosity and Brownian rotation) and allows an evaluation of the differential thermodynamic parameters, $\Delta\Delta H°$ and $T\Delta\Delta S°$, from the slope and intercept, respectively. For example, in the case of DBTA with β-cyclodextrin, $\Delta\Delta H° = -6.37$ kJ/mol and $T\Delta\Delta S° = -6.03$ kJ/mol, indicating that the

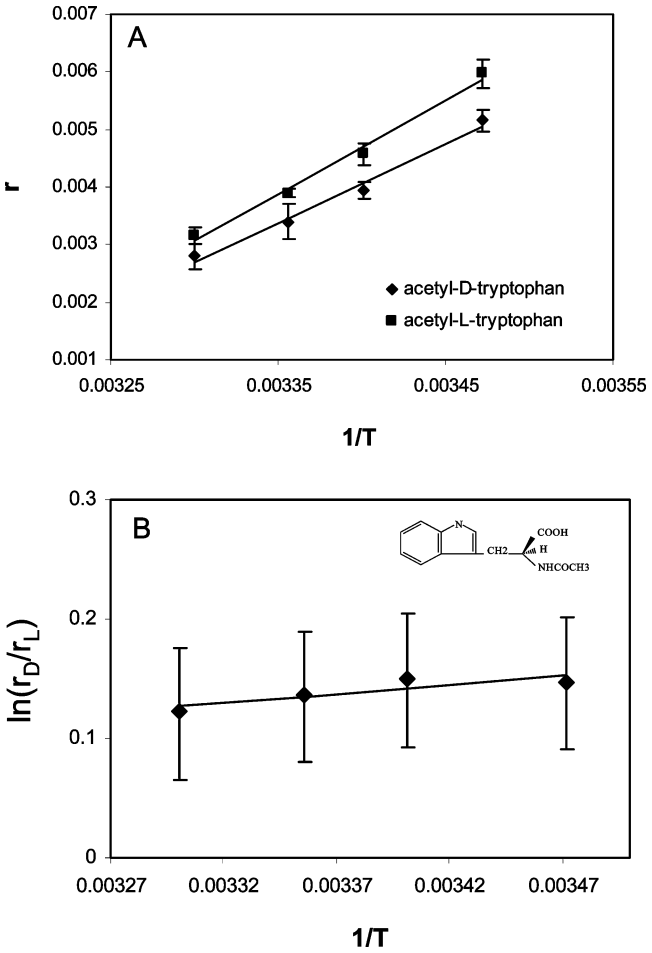

Figure 6. Temperature-dependent fluorescence anisotropy of the enantiomers of *N*-acetyl tryptophan in the presence of β-cyclodextrin shown as the anisotropy values (A) and the natural logarithm of the ratio of anisotropy values for the enantiomers (B).

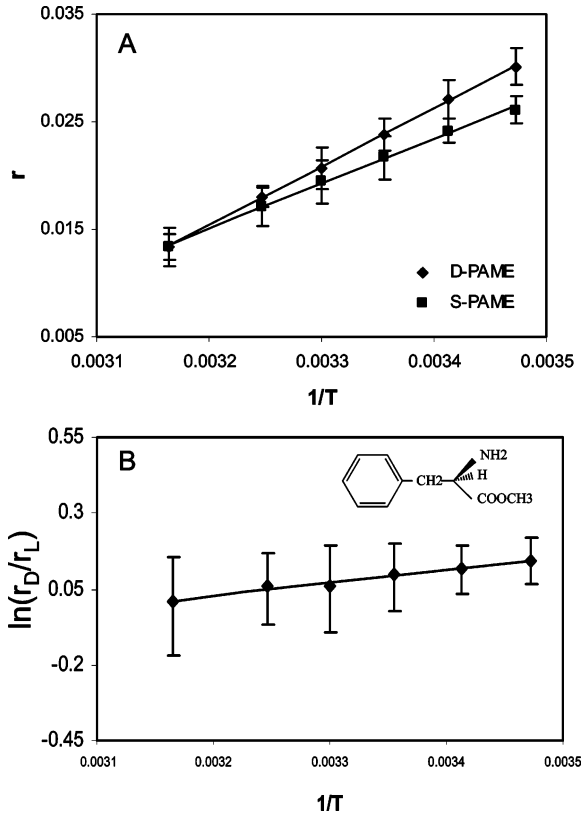

Figure 7. Temperature-dependent fluorescence anisotropy of the phenylalanine methyl ester (PAME) in the presence of β-cyclodextrin shown as the anisotropy values (A) and the natural logarithm of the ratio of anisotropy values for the enantiomers (B).

discrimination mechanism ($\Delta\Delta G° = -0.33$ kJ/mol) is driven primarily by enthalpic considerations.

Figures 2−4 show the results for a series of binaphthyl analogues. These compounds are atrope isomers because their chirality is defined by a chiral plane rather than a chiral center. The differences in the series result from the polar functional groups (phosphate, amine, or alcohol) and the variation in the dihedral angle of the naphthyl moieties. All three analogues examined exhibited evidence of similar recognition mechanisms, as evidenced by entropy-dominated chiral recognition. This can be inferred from the fact that the magnitude of $T\Delta\Delta S°$ is greater than that of $\Delta\Delta H°$ in each case. Figure 2 shows the fluorescence anisotropy data obtained for the enantiomers of BNP. Studies based on circular dichroism reported a dihedral angle of ~55° between the naphthylene moieties.[44] Multiple mechanisms are possible for forming inclusion complexes with β-CD, whereby BNP could approach the cyclodextrin cavity through one of the two naphthyl rings or even the phosphate group.[18] Geometric considerations dictate that both naphthyl moieties cannot simultaneously occupy the CD cavity. It is likely that one naphthyl moiety occupies the cyclodextrin cavity, which would result in significant interactions between the outer surface of the cyclodextrin and the other naphthyl moiety, disrupting the solvation environment of cyclodextrin to a larger degree than complex formation simply involving the hydrophobic core. In contrast to DBTA, the temperature response shown in Figure 2b has a negative slope, indicating greater chiral recognition at higher temperatures. This observation is in general agreement with literature values obtained by thermodynamic studies[18] and by CE experiments in our laboratory (Figure 2b inset). The large anisotropy ratios observed correspond to the chiral selectivity of β-CD toward BNP at all temperatures examined, which is also evidenced by a relatively large $\Delta\Delta G°$. Data obtained for BNA and BOH are shown in Figures 3 and 4. The $\Delta\Delta H°$ and $T\Delta\Delta S°$ values are significantly larger in the cases of BNA and BOH, compared to BNP, although the differences are largely compensatory and result in small $\Delta\Delta G°$ values (Table 1). The trend observed in selectivity corresponds to the polarity of the polar moiety.

β-CD serves as a model for chiral recognition of amino acids. Recently, several methods have been utilized in studies of the β-CD inclusion complexes of amino acids as well as their derivatives including microcalorimetry, UV−vis spectroscopy and mass spectrometry.[3−5,11] In this work, phenylalanine methyl ester (PAME), *N*-acetyl tryptophan, and tryptophan were chosen to demonstrate the ability of fluorescence anisotropy measurements to study molecular recognition and chiral discrimination of amino acid derivatives. Figures 5−7 show the data obtained for tryptophan, *N*-acetyl tryptophan, and PAME, respectively. Positive slopes observed in Figures 5b, 6b, and 7b indicate an enthalpically driven chiral selectivity in all three cases, as borne out by the fact that the magnitude of $\Delta\Delta H°$ is greater than that of $T\Delta\Delta S°$ (Table 1).

Figure 8 shows the temperature response of the fluorescence anisotropy for the hypertension drug propranolol in the presence of β-cyclodextrin. Similar to the binaphthyl compounds, differences in anisotropy values between two enantiomers are greatest at higher temperatures (Figure 8). A positive $\Delta\Delta H°$ value of 10.82 kJ/mol is observed. The magnitude of $T\Delta\Delta S°$ is even larger, indicating an entropically driven process. Assuming

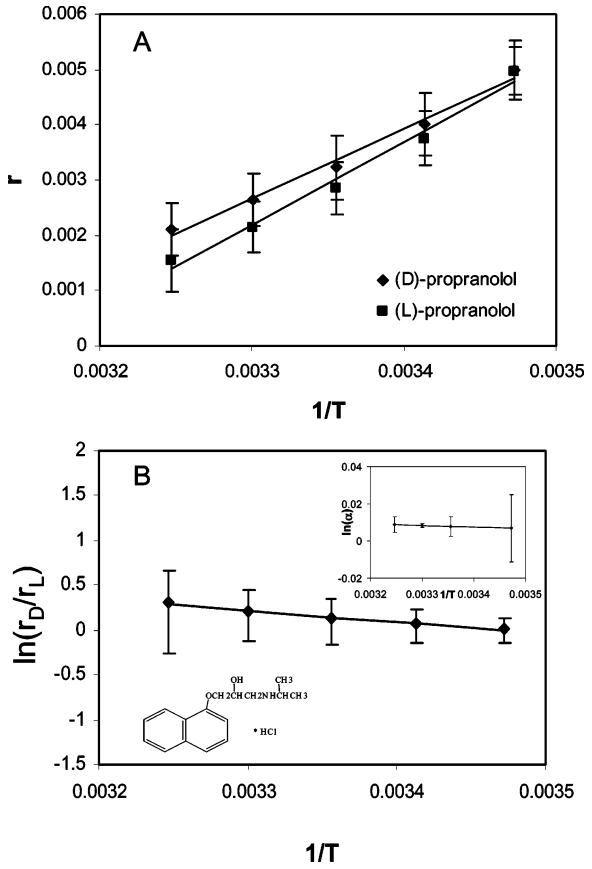

Figure 8. Temperature-dependent fluorescence anisotropy of the enantiomers of propranolol in the presence of β-cyclodextrin shown as the anisotropy values (A) and the natural logarithm of the ratio of anisotropy values for the enantiomers (B). The inset shows data obtained from CE measurements.

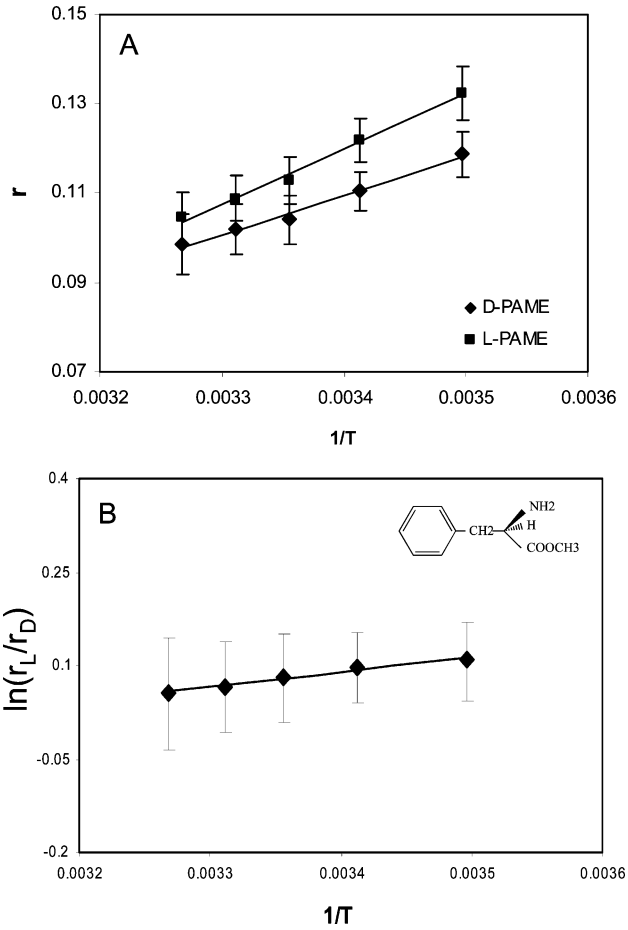

Figure 9. Temperature-dependent fluorescence anisotropy of the enantiomers of phenyl alanine methyl ester (PAME) in the presence of poly(sodium undecanoyl-L-valinate) (PSUV) shown as the anisotropy values (A) and the natural logarithm of the ratio of anisotropy values for the enantiomers (B).

the naphthyl moiety penetrates the hydrophobic cyclodextrin core, it can be deduced that during the binding event the chiral center is relatively distant from the chiral selector, which may be responsible for the low chiral selectivity in β-cyclodextrin. Chromatographic separation of the propranolol enantiomers has been performed by high performance liquid chromatography (HPLC), and a relatively small chiral selectivity was reported ($\alpha = 1.04$);[14] studies using microcalorimetry also reported association constants that did not differ beyond measurement error.[5] The experimental results were confirmed by capillary electrophoresis measurements in our laboratory showing similar trends under the same conditions (Figure 8a inset).

Poly(sodium undecanoyl-L-valinate). The interactions of the enantiomers of four chiral compounds with the molecular micelle poly(sodium undecanoyl-L-valinate) (PSUV) were also investigated. Poly(sodium undecanoyl-L-valinate) is a molecular micelle (polymeric micelle) composed of surfactant monomers that are covalently linked within the hydrophobic core of the micelle.[43] The hydrophilic headgroups are composed of the amino acid, valine, in a c-terminal configuration. The analyte polarity and charge state play important roles in governing complexation and chiral recognition processes in this system. The most significant factor that determines the analyte−polymer interactions is the solubility of the analyte in the solvent system. Other factors such as specific ionic and/or hydrogen bonding interactions play an additional role in governing the binding interactions and can lead to chiral discrimination.

Figure 9 shows the temperature dependence of the fluorescence anisotropy and the anisotropy ratio for PAME with PSUV. Compared to the results obtained with β-CD, this system exhibits much higher anisotropy values for both PAME enantiomers primarily because of the larger size of the micelle polymer relative to the cyclodextrin. Contrary to the case of β-CD, PSUV shows greater affinity for the L enantiomer of PAME. The smaller anisotropy ratio (compared to that of β-CD) indicates poorer chiral recognition for PSUV toward PAME enantiomers. This can be understood by considering PAME's structural features. At a pH of 9.0, PAME does not bear any charge, resulting in a loss of electrostatic interaction as a mode of interaction with PSUV. Thus, the decrease in solubility and the lack of ionic interactions with the carboxylic acid group of PSUV likely result in significant penetration of the analyte into the achiral hydrophobic core of the molecular micelle and a lower chiral selectivity.

The interactions of DBTA were also examined with PSUV (Figure 10). Although the magnitude of the anisotropy was larger than that in the case of β-CD, as was observed in PAME, an anomalous trend was observed. The anisotropy decreased smoothly with increased temperature between 16 and 30 °C, but at temperatures above 30 °C the anisotropy actually increased slightly. This trend could be associated with a structural change in the molecular micelle at higher temperatures (above 35 °C), but no such phenomenon was observed in the case of PAME. Alternatively, if the solubility of the diprotic DBTA varies significantly with temperature, then a marked increase in the steady-state anisotropy values could be observed because of a shift in the complex equilibrium. The exact cause of this curious behavior remains elusive and is

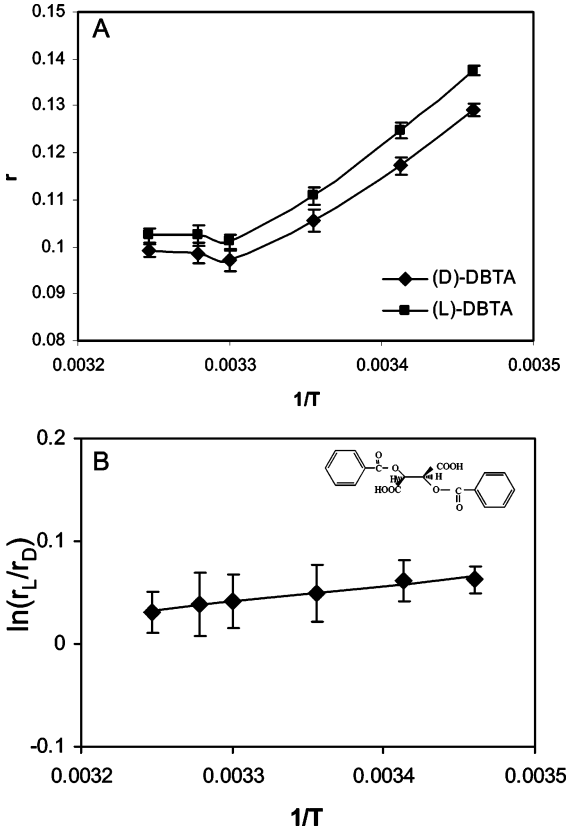

Figure 10. Temperature-dependent fluorescence anisotropy of the enantiomers of O,O′-dibenzoyl tartaric acid (DBTA) in the presence of poly(sodium undecanoyl-L-valinate) (PSUV) shown as the anisotropy values (A) and the natural logarithm of the ratio of anisotropy values for the enantiomers (B).

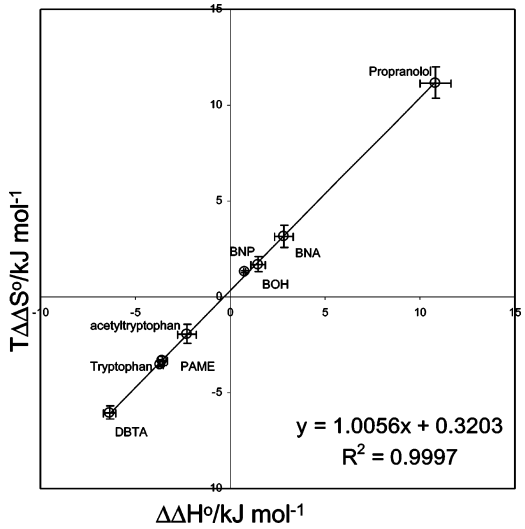

Figure 11. Enthalpy−entropy compensation plots for β-cyclodextrin.

currently under investigation in our laboratory. Most interesting in the current study, however, is the fact that the chiral recognition process does not appear to be affected to a significant degree by the phenomenon, as evidenced by the trend observed in Figure 10b. Linearity is not as good as in other cases ($R^2 = 0.96$) but does not show any correlation with the anomaly observed in Figure 10a. This case illustrates that the developed method is rather insensitive to nonstereoselective artifacts.

Enthalpy−Entropy Compensation Plots. Enthalpy−entropy compensation is an interesting phenomenon that is

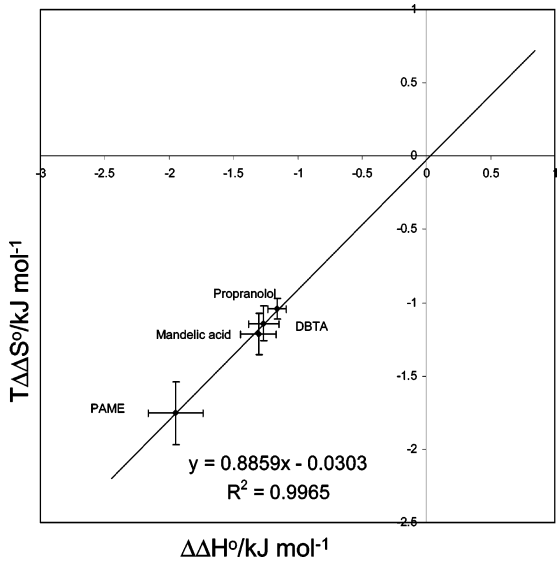

Figure 12. Enthalpy−entropy compensation plots for poly(sodium undecanoyl-L-valinate).

widely observed in various reactions.[45,46] A recent study by Rekharsky and Inoue details compensatory enthalpy−entropy relationships for over 40 enantiomer pairs with β-CD. A general conclusion reported is that for complexation processes, compensatory plots generated from relatively small data sets (~50 enantiomer pairs) tend to have such scattered data that the slope of the line could yield erroneous conclusions.[5] It was reported, however, that good compensatory enthalpy−entropy relationships were obtained for chiral recognition processes based on differential enthalpy and entropy for enantiomeric pairs. Because the method developed in this study inherently produces differential thermodynamic parameters, compensatory enthalpy−entropy relationships were evaluated for the enantiomer pairs examined. Figures 11 and 12 show the enthalpy−entropy compensation plots obtained for several enantiomers pairs with β-CD and PSUV. Although there is debate concerning the accuracy and interpretation of enthalpy−entropy compensation plots (they can be wrought with measurement artifacts), it is nevertheless interesting that excellent enthalpy−entropy compensation relationships are observed with very little scatter ($R^2 = 0.9997, 0.996$) and the results are generally consistent with literature values.[5]

More important and useful is the observation that the analytes are grouped in the plot according to general structure. Namely, the three binaphthyl analogues examined appear as one group, and the amino acid-based species appear as another. The hypertension drug propranolol, which has a unique structure compared to that of the other analytes, is isolated in the plot. Thus, the enthalpy−entropy compensation plot allows a qualitative assessment of the mode of chiral discrimination. Although still linear, the compensatory plot obtained in the case of the molecular micelle is rather different than in the case of the β-CD. The three analytes that were examined (PAME, DBTA, and propranolol) with both chiral selectors show no clear correlation between the two cases, as might be expected on the basis of the different structures and modes of enantiodiscrimination.

Conclusions

It has been demonstrated that fluorescence anisotropy holds significant potential as a technique for examining chiral recognition. We have shown that fluorescence anisotropy is a sensitive tool that can be used to study the subtle effect of chiral

recognition. We have shown from fundamental principles that the steady-state fluorescence anisotropy of enantiomer pairs interacting with a chiral selector is related to the thermodynamic parameters of enantioselective binding because of the additive nature of polarization measurements (eq 3) and the direct relationship between the host−guest association equilibrium and the fraction of bound species. Equation 15 predicts a linear relationship that is clearly evidenced in Figures 1−10. Figures 11 and 12 show the differential entropy and enthalpy determined for the analytes in the case of β-CD and PSUV. In some cases, discrepancies exist between the determined differential thermodynamic parameters and those reported in the literature. These discrepancies are currently under investigation in our laboratory. It is worth noting the method developed in this study directly produces $\Delta\Delta H°$ and $T\Delta\Delta S°$ values with a precision that is significantly better than that of microcalorimetry and $\Delta\Delta G°$ values with errors generally comparable to those of microcalorimetry. Thus, fluorescence anisotropy is demonstrated to be a complementary tool in the small arsenal of techniques capable of examining chiral recognition and the thermodynamics of enantiodiscrimination.

Acknowledgment. We gratefully acknowledge support from the donors of the Petroleum Research Fund, administered by the American Chemical Society (PRF no. 39264-G4) and the SIU Materials Technology Center. Additional support for this research was provided by Southern Illinois University in the form of startup funds and the Faculty Seed Grant Program. We also thank Janice M. Clements (SIU) and Isiah M. Warner (LSU) for assistance in the synthesis and polymerization of the molecular micelle examined in the study.

References and Notes

(1) Stinson, S. C. *Chem. Eng. News* **2001**, *79*, 45−56.
(2) Maier, N. M.; Franco, P.; Lindner, W. *J. Chromatogr., A* **2001**, *906*, 3−33.
(3) Liu, Y.; Zhang, Y.; Sun, S.; Li, Y.; R, C. *J. Chem. Soc., Perkin Trans. 2* **1997**, 1275−1278.
(4) Liu, Y.; Zhang, Y.; Sun, S.; Li, Y.; R., C. *J. Chem. Soc., Perkin Trans. 2* **1997**, 1609−1613.
(5) Rekharsky, M.; Inoue, Y. *J. Am. Chem. Soc.* **2000**, *122*, 4418−4435.
(6) Rekharsky, M. V.; Inoue, Y. *J. Am. Chem. Soc.* **2002**, *124*, 813−826.
(7) Kurtan, T.; Nesnas, N.; Koehn, F. E.; Li, Y. Q.; Nakanishi, K.; Berova, N. *J. Am. Chem. Soc.* **2001**, *123*, 5974−5982.
(8) Kurtan, T.; Nesnas, N.; Li, Y. Q.; Huang, X.; Nakanishi, K.; Berova, N. *J. Am. Chem. Soc.* **2001**, *123*, 5962−5973.
(9) Clark, J. L.; Stezowski, J. J. *J. Am. Chem. Soc.* **2001**, *123*, 9880−9888.
(10) Clark, J. L.; Booth, B. R.; Stezowski, J. J. *J. Am. Chem. Soc.* **2001**, *123*, 9889−9895.
(11) Lipkowitz, K. B.; Raghothama, S.; Yang, J. *J. Am. Chem. Soc.* **1992**, *114*, 1554−1562.
(12) Maletic, M.; Wennemers, H.; McDonald, D. Q.; Breslow, R.; Still, W. C. *Angew. Chem., Int. Ed. Engl.* **1996**, *35*, 1490−1492.
(13) Zhang, J. Z. *Acc. Chem. Res.* **1997**, *30*, 424.
(14) Armstrong, D. W.; Ward, T. J.; Armstrong, R. D.; Beesley, T. E. *Science* **1986**, *232*, 1132−1135.
(15) Pirkle, W. H.; Murray, P. G. *J. Org. Chem.* **1996**, *61*, 4769−4774.
(16) Fornstedt, T.; Gotmar, G.; Anderson, M.; Guiochen, G. *J. Am. Chem. Soc.* **1999**, *121*, 164−1674.
(17) Yashima, E.; Yamamoto, C.; Okamoto, Y. *J. Am. Chem. Soc.* **1996**, *118*, 4036−4048.
(18) Kano, K.; Kato, Y.; Kodera, M. *J. Chem. Soc., Perkin Trans. 2* **1996**, 1211−1217.
(19) Lammerhofer, M.; Peters, E. C.; Yu, C.; Svec, F.; Frechet, J. M. J.; Lindner, W. *Anal. Chem.* **2000**, *72*, 4614−4622.
(20) Yarabe, H. H.; Shamsi, S.; Warner, I. M. *Anal. Chem.* **1999**, *71*, 3992−3999.
(21) Chankveltadze, B. *Capillary Electrophoresis in Chiral Analysis*; John Wiley & Sons: West Sussex, U.K., 1997; pp 141−222.
(22) McCarroll, M. E.; Haddadian, F.; Warner, I. M. *J. Am. Chem. Soc.* **2001**, *123*, 3173−3174.
(23) Pu, L. *Chem. Rev.* **2004**, *104*, 1687−1716.
(24) James, T. D.; Sandanayake, K.; Shinkai, S. *Nature* **1995**, *374*, 345−347.
(25) Corradini, R.; Sartor, G.; Marchelli, R.; Dossena, A. *J. Chem. Soc., Perkin Trans.* **1992**, 1979−1983.
(26) Al Rabaa, A. R.; Tfibel, F.; F., M.; Pernot, P.; Fontaine-Aupart, M. *J. Chem. Soc., Perkin Trans. 2* **1999**, 341−352.
(27) Ouchi, A.; Zandomeneghi, G.; Zandomeneghi, M. *Chirality* **2002**, *14*, 1−11.
(28) Lynam, C.; Jennings, K.; Nolan, K.; Kane, P.; McKervey, M. A.; Diamond, D. *Anal. Chem.* **2002**, *74*, 59−66.
(29) Lin, J.; Hu, Q.-S.; Xu, M.-H.; Pu, L. *J. Am. Chem. Soc.* **2002**, *124*, 2088−2089.
(30) Yan, Y.; Myrick, M. L. *Anal. Chem.* **1999**, *71*, 1958−1962.
(31) Kumar, C. V.; Buranaprapuk, A.; Opiteck, G. J.; Moyer, M. B.; Jockusch, S.; Turro, N. J. *Proc. Natl. Acad. Sci. U.S.A.* **1998**, *95*, 10361−10366.
(32) Pagliari, S.; Corradini, R.; Galaverna, G.; Sforza, S.; Dossena, A.; Marchelli, R. *Tetrahedron Lett.* **2000**, *41*, 3691−3695.
(33) Hayashida, O.; Ono, K.; Hisaeda, Y.; Murakami, Y. *Tetrahedron* **1995**, *51*, 8423−8436.
(34) Xu, Y.; McCarroll, M. E. *J. Phys. Chem. A* **2004**, *108*, 6929−6932.
(35) Lakowicz, J. R. *Principles of Fluorescence Spectroscopy*; Plenum: New York, 1983.
(36) Easton, C. J.; Lincoln, S. F. *Chem. Soc. Rev.* **1996**, *25*, 163−170.
(37) Szejtli, J. *Chem. Rev.* **1998**, *98*, 1743−1753.
(38) Breslow, R.; Dong, S. D. *Chem. Rev.* **1998**, *98*, 1997−2011.
(39) Harata, K. *Chem. Rev.* **1998**, *98*, 1803−1827.
(40) Rekharsky, M. V.; Inoue, Y. *Chem. Rev.* **1998**, *98*, 1875−1917.
(41) Uekama, K.; Hirayama, F.; Irie, T. *Chem. Rev.* **1998**, *98*, 2045−2076.
(42) Rekharsky, M.; Inoue, Y. *J. Am. Chem. Soc.* **2000**, *122*, 10949−10955.
(43) Wang, J.; Warner, I. M. *Anal. Chem.* **1994**, *66*, 3773−3776.
(44) Setnicka, V.; Urbanova, M.; Bour, P.; Kral, V.; Volka, K. *J. Phys. Chem. A* **2001**, *105*, 8931−8938.
(45) Leffler, J. E. *J. Org. Chem.* **1955**, *20*, 1202−1231.
(46) Grunwald, E.; Steel, C. *J. Am. Chem. Soc.* **1995**, *117*, 5687−5692.